7 Tesla Chlorine (^{35}Cl) and Sodium (^{23}Na) MR Imaging of an Enchondroma

7 Tesla Chlor (^{35}Cl) und Natrium (^{23}Na) MR-Bildgebung eines Enchondroms

Authors

Marc-André Weber[1, 2], Lisa Seyler[3], Armin M. Nagel[3, 4]

Affiliations

1 Clinic of Diagnostic and Interventional Radiology, University Hospital Heidelberg, Heidelberg, Germany
2 Institute of Diagnostic and Interventional Radiology, Pediatric Radiology and Neuroradiology, University Medical Center Rostock, Rostock, Germany
3 Institute of Radiology, University Hospital Erlangen, Friedrich-Alexander-Universität Erlangen-Nürnberg (FAU), Erlangen, Germany
4 Medical Physics in Radiology, German Cancer Research Center (DKFZ), Heidelberg, Germany

published online 12.08.2021

Bibliography

Fortschr Röntgenstr 2021; 193: 1207–1211

DOI 10.1055/a-1472-6730

ISSN 1438-9029

Georg Thieme Verlag KG, Rüdigerstraße 14, 70469 Stuttgart, Germany

Correspondence

Herr Prof. Marc-André Weber
Universitätsmedizin Rostock, Diagnostische und Interventionelle Radiologie, Kinder- und Neuroradiologie, Ernst-Heydemann-Str. 6, D-18057 Rostock, Germany
Tel.: +49/3 81/4 94 92 01
Fax: +49/3 81/4 94 92 02
marc-andre.weber@med.uni-rostock.de

ZUSAMMENFASSUNG

Wir zeigen die Machbarkeit der 7-Tesla Natrium (^{23}Na–) und Chlor (^{35}Cl)-MRT eines solitären Enchondroms. Zu diesem Zweck haben wir spezielle Sequenzen auf einem 7-Tesla-Ganzkörpersystem mit den folgenden Parametern etabliert: für die ^{35}Cl-MRT TE/TR = 0,35/60 ms, T_{RO} = 5 ms, α = 90°, Δx^3 = (6 mm)^3, 3 Mittelungen, T_{acq} = 30 min und für ^{23}Na-MRT TE/TR = 0,4/101 ms, T_{RO} = 10 ms; α = 90°; Δx^3 = (1,9 mm)^3, 3 Mittelungen, T_{acq} = 30 min 18 s. Die gemessene scheinbare Na^+-Konzentration betrug 255 mmol/l und war etwa 7-fach höher als die scheinbare Cl^--Konzentration mit etwa 36 mmol/l. Darüber hinaus zeigten wiederholte Protonen-MRT-Untersuchungen über 14 Jahre ein konstantes, geringes Wachstum (≈ 0,65 ml/Jahr). Zusammenfassend lässt sich sagen, dass Enchondrome im Vergleich zum normalen Knochenmark in der ^{23}Na- und ^{35}Cl-MRT offensichtlich ein hohes Kontrast-Rausch-Verhältnis aufweisen, was in unklaren oder subtilen Fällen zur Erkennung und Differenzierung beitragen kann.

Kernaussagen:

- Hohe Magnetfeldstärken (z. B. 7 Tesla) ermöglichen Natrium (^{23}Na) und Chlor (^{35}Cl) MRT von solitären knorpelbildenden Tumoren wie Enchondromen mit nominellen räumlichen Auflösungen von (1,9 mm)^3 (^{23}Na-MRT) und (6 mm)^3 (^{35}Cl-MRT).
- Die medianen scheinbaren Konzentrationen von Na^+ und Cl^- in einemsolitären Enchondrom waren fast 13-fach bzw. 3-fach höher als in normalem Muskelgewebe.
- Enchondrome weisen im Vergleich zum normalen Knochenmarkbei 23Na- und 35Cl-MRT ein hohes Kontrast-Rausch-Verhältnis auf, das in unklaren oder subtilen Fällen zur besseren Erkennung und Differenzierung beitragen kann.

ABSTRACT

We demonstrated the feasibility of 7 Tesla sodium (^{23}Na) and chlorine (^{35}Cl) MRI of a solitary enchondroma. For this, we established dedicated sequences on a 7-Tesla whole-body system with the following key parameters for ^{35}Cl MRI: TE/TR = 0.35/60 ms, T_{RO} = 5 ms, α = 90°, Δx^3 = (6 mm)^3, 3 averages, T_{acq} = 30 min and for ^{23}Na MRI: TE/TR = 0.4/101 ms, T_{RO} = 10ms; α = 90°; Δx^3 = (1.9 mm)^3, 3 averages, T_{acq} = 30 min 18 s. The measured apparent Na^+ concentration was 255 mmol/l and was approximately 7-fold higher than the apparent Cl^- concentration with about 36 mmol/l. Additionally, repeated proton MRI examinations demonstrated constant but subtle growth (≈ 0.65 ml/year) over 14 years. In conclusion, enchondromas obviously have a high contrast-to-noise ratio when compared with the normal bone marrow in ^{23}Na and ^{35}Cl MRI, which may contribute to detection and differentiation in unclear or subtle cases.

Thieme

Key Points:

- High magnetic field strengths (e. g., 7 Tesla) enable sodium (^{23}Na) and chlorine (^{35}Cl) MRI of solitary cartilage-forming tumors like enchondromas with nominal spatial resolutions of (1.9 mm)^3 (^{23}Na MRI) and (6 mm)^3 (^{35}Cl MRI).
- Measured median tumoral apparent Na^+ and Cl^- concentrations were nearly 13 times higher and 3 times higher than in normal muscle tissue, respectively.
- Enchondromas have a high contrast-to-noise-ratio when compared with the normal bone marrow in ^{23}Na and ^{35}Cl MRI, which may contribute to detection and differentiation in unclear or subtle cases.

Citation Format

- Weber M, Seyler L, Nagel AM. 7 Tesla Chlorine (^{35}Cl) and Sodium (^{23}Na) MR Imaging of an Enchondroma. Fortschr Röntgenstr 2021; 193: 1207–1211

Introduction

Ultra-high field magnetic resonance imaging (MRI) (e. g., 7 Tesla) enables increased signal-to-noise ratio and, thus, also efficient detection of elements other than hydrogen such as sodium (^{23}Na), chlorine (^{35}Cl), potassium (^{39}K), and oxygen (^{17}O) [1]. Recently, ^{35}Cl together with ^{23}Na MRI on a 7 Tesla whole-body MRI system could be implemented for evaluating human muscle and brain tissue in vivo [2, 3]. The Na^+ content in healthy articular cartilage is the highest among all tissues with reported values of ≈240–260 mmol/l. The fixed negative charge density on the glycosaminoglycan side chains within the cartilage tissue attracts Na^+ ions [4]. Glycosaminoglycans are a key element of the proteoglycan matrix of cartilage tissue. Chloride (Cl^-) is the most abundant anion in the human body and influences cellular osmolarity and thereby cell volume [2]. Until now, the Na^+ and Cl^- concentration of chondroid tumors have not been measured noninvasively in vivo.

Chondroid tumors are a heterogeneous group of neoplasms that all share the production of chondroid matrix. Benign chondroid tumors are some of the most common incidental bone lesions, with the mostly asymptomatic enchondroma representing the second most common primary bone tumor (3–10 % of all bone tumors, 12–14 % of all benign bone tumors). The malignant counterpart, chondrosarcoma, is the second most common malignant primary bone tumor. Up to 65 % of all enchondromas are observed in the small tubular bones of the hand, but they are also encountered in 3 % of all routine knee MRI scans and 2 % of all routine shoulder MRI scans, often with a central location within the medullary cavity of the bone and localized metaphyseal or metadiaphyseal [5, 6]. Enchondromas are on the one hand frequent incidental MRI findings and on the other hand have the potential for malignant transformation to chondrosarcoma. In a retrospective study, 4 % of solitary enchondromas changed into chondrosarcoma after 4 to 12 years [7]. Moreover, it may be difficult to distinguish an enchondroma from a low-malignant chondrosarcoma by imaging as well as histopathologically. Therefore, enchondromas are often mostly followed with regard to growth and/or changes indicating aggressive tumor, and Danish guidelines regarding when, how, and how long to follow enchondromas with regard to malignant transformation were recently published [6]. Regarding the differentiation of enchondroma from low-malignant chondrosarcoma or atypical cartilage tumors, more advanced MRI techniques such as dynamic contrast-enhanced MRI [8] and MRI-based three-dimensional texture analysis using parameters like kurtosis [9] have been proposed. However, differentiation remains challenging, and all criteria published until present are not absolutely specific [5].

In this study, we used a 7 Tesla MRI system to demonstrate the feasibility of ^{35}Cl and ^{23}Na MRI for characterizing a cartilage tumor, such as an enchondroma. Moreover, apparent Na^+ and Cl^- concentrations were quantified, since these concentrations largely depend on the type of tissue and are often altered in tumor tissue [2, 10]. In addition, chloride channels have been reported to be involved in cell migration in gliomas [11].

Materials and Methods

^{23}Na and ^{35}Cl MRI were implemented on a 7.0 Tesla whole-body system (Magnetom 7 T, Siemens Healthineers, Erlangen, Germany). The 7 Tesla MRI system was equipped with double-resonant ^{35}Cl/^{1}H and ^{23}Na/^{1}H birdcage radiofrequency (RF) coils (QED, Mayfield Village, Ohio, USA and RAPID Biomedical, Rimpar, Germany). The RF coils had inner diameters of 22 cm (^{35}Cl/^{1}H coil) and 26 cm (^{23}Na/^{1}H coil). The 7 Tesla MRI system and the RF coils were operated as investigational devices. Supervision of the specific absorption rate (SAR) was implemented by the manufacturer. A custom-written three-dimensional density-adapted projection reconstruction sequence was applied for 7 Tesla [2, 3] that was originally developed for 3 Tesla ^{23}Na MRI [12]. To minimize relaxation weighting, the following parameters were used: ^{23}Na MRI (TE (echo time)/TR (repetition time) = 0.4/101 ms, T_{RO} = 10ms; flip angle $\alpha = 90°$; $\Delta x^3 = (1.9\,mm)^3$, 3 averages, T_{acq} = 30 min 18 s); ^{35}Cl MRI (TE/TR = 0.35/60 ms, T_{RO} = 5 ms, $\alpha = 90°$, $\Delta x^3 = (6\,mm)^3$, 3 averages, T_{acq} = 30 min). Image reconstruction was performed offline using Matlab (MathWorks, Natick, Mass). Apparent Na^+ concentrations and apparent Cl^- concentrations were estimated in the cartilage-forming tumor using reference tubes containing NaCl solution and agarose gel. ROIs were placed in each reference phantom and a linear regression was performed.

In addition, repeated proton MRI examinations (▶ **Fig. 1**) were performed over a time period of 14 years and tumor volume was manually segmented for all slices with the help of Medical Interaction Toolkit (MITK) [13]. For the segmentation mainly isotropic T1-weighted gradient echo sequences with submillimeter spatial resolution were used. No image registration was performed.

Written informed consent was obtained from the male subject, who has participated in MRI research studies as a healthy volunteer between the ages of 27 and 41 years for sequence optimization.

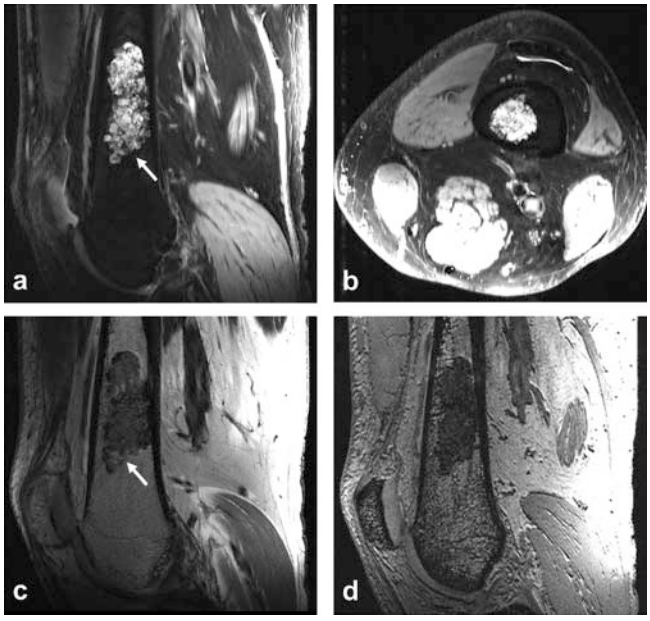

▶ **Fig. 1** Illustration of the MRI findings (after 14 years). 7 Tesla ^{1}H MR images (**a**, sagittal proton density (PD)-weighted, fat-saturated MRI (TR/TE = 6230/12 ms), **b** transverse PD fat-saturated MRI (8730/12 ms), sagittal T1-weighted spin-echo MRI (TR/TE = 1600/9.6 ms) **c** and high-resolution (0.45 mm)^3 T1-weighted gradient-echo MRI **d**). The arrows point to the enchondroma in the distal femur.

▶ **Abb. 1** Illustration von MRT Befunden (nach 14 Jahren). 7 Tesla ^{1}H MRT Aufnahmen (**a**, sagittale Protondendichte (PD) gewichtete, fettsupprimierte Sequenz (TR/TE = 6230/12 ms), **b** transversale PD-gewichtete, fettsupprimierte Sequenz (8730/12 ms), sagittale T1-gewichtete Spinechosequenz (TR/TE = 1600/9,6 ms) **c** und hochauflösende (0,45 mm)^3 T1-gewichtete Gradientenechosequenz **d**). Die Pfeile deuten auf das Enchondrom im distalen Femur.

Results

Morphological MRI revealed a poly-lobulated lesion within the left distal femur (▶ **Fig. 1**). The lesion has a typical imaging aspect of an enchondroma with low signal intensity on T1-weighted and high signal intensity on T2-weighted MR images. No peritumoral bone marrow edema or cortical abutment or penetration was diagnosed during the observation period. An additional nuclear bone scan demonstrated a solitary slight tracer uptake of the lesion without any hints of additional lesions (not shown). The proton MRI examinations demonstrated slight but constant tumor growth (▶ **Fig. 2**). A linear interpolation shows that the volume of the enchondroma increased by approximately 0.65 cm^3 per year.

^{35}Cl and ^{23}Na MRI of the enchondroma revealed acceptable image quality (▶ **Fig. 3**). The apparent Na^+ concentration of the enchondroma was 255 mmol/l and approximately 7-fold higher than the apparent Cl^- concentration (36 mmol/l), whereas the apparent Na^+ and Cl^- concentration of the cancellous and cortical bone was equal to background noise (▶ **Fig. 3**).

Discussion

The measured apparent Na^+ concentration in the cartilage forming enchondroma is similar to the apparent Na^+ concentration in healthy articular cartilage. Compared to muscle tissue of healthy volunteers with a mean muscular apparent Na^+ concentration in mmol/l of 19.9 ± 1.9 and an apparent Cl^- concentration of 12.2 ± 1.6 [3], the measured apparent Na^+ and Cl^- concentrations within the enchondroma were substantially higher. An increased apparent chlorine concentration has been reported in glioma tissue of humans using 7 Tesla [2] substantiating the hypothesis of the

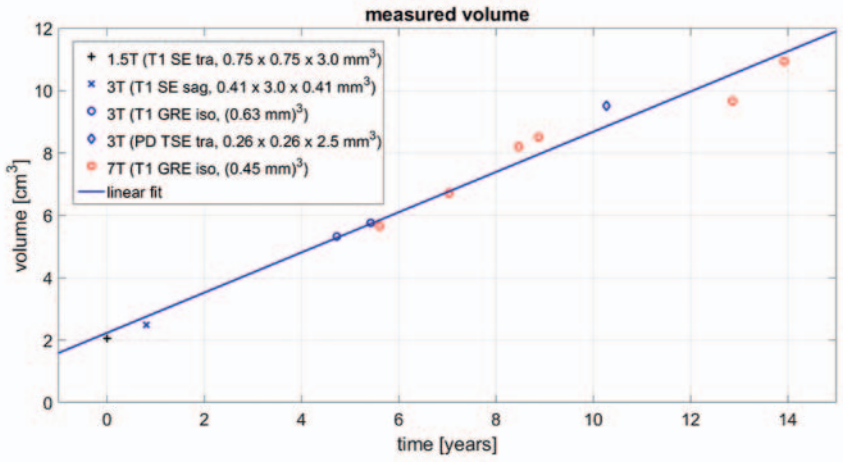

▶ **Fig. 2** Growth of the enchondroma over a period of 14 years. The volume of the enchondroma increases approximately linearly with time. Linear interpolation revealed a growth rate of 0.65 cm^3 per year. Different types of pulse sequences, as indicated in the figure inset, were used for the volumetric analysis.

▶ **Abb. 2** Wachstum des Enchondroms über einen Zeitraum von 14 Jahren. Das Volumen des Enchondroms wächst annähernd linear mit der Zeit. Die lineare Interpolation zeigt eine Wachstumsrate von 0,63 cm^3 pro Jahr. Verschiedene Arten von Pulssequenzen, wie in dem Bild dargestellt, wurden für die volumetrische Analyse verwendet.

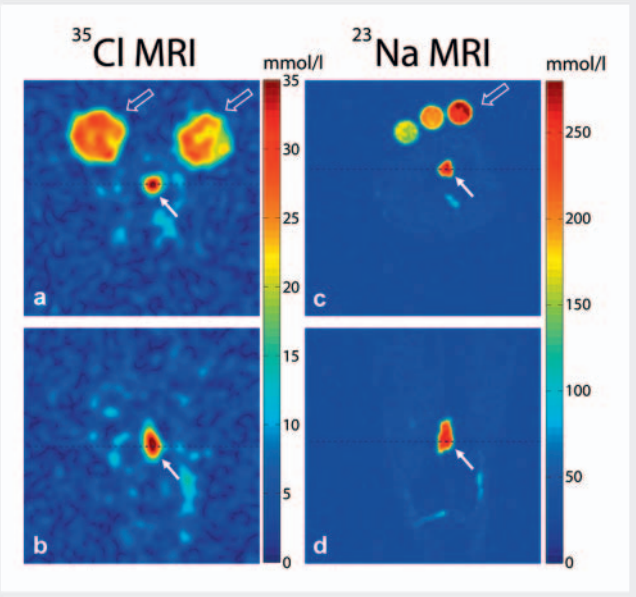

▶ **Fig. 3** Selected transverse **a, c** and coronary slices **b, d** of 3 D $^{35}Cl^-$ and ^{23}Na-data sets of the enchondroma (after 6 years). The positions of the different slices are indicated by dotted lines. Note that no co-registration of the $^{35}Cl^-$ and ^{23}Na-data sets was performed. Nominal spatial resolutions of $(6\,mm)^3$ (^{35}Cl MRI, **a, b**) and $(1.9\,mm)^3$ (^{23}Na MRI, **c, d**) were achieved. The measured apparent sodium concentration (255 mmol/l) of the enchondroma is approximately 7-fold higher than the apparent chlorine concentration (36 mmol/l). The Na^+ and Cl^- color bars are differently scaled. Three reference phantoms (open arrow) containing 5 % agarose gel and differently concentrated NaCl solutions (**c** (Na^+) = 154/205/257 mmol/L) are visible in ^{23}Na MRI and two reference phantoms (**c** (Cl^-) = 26 mmol/L; left: 4 % agarose gel; right: without agarose gel) are also visible in the ^{35}Cl MR image (open arrows).

▶ **Abb. 3** Ausgewählte transversale **a, c** und koronale Schichten **b, d** der 3 D $^{35}Cl^-$ und ^{23}Na-Datensätze des Enchondroms (nach 6 Jahren). Die Positionen der verschiedenen Schichten sind als gepunktete Linien angezeigt. Es wurde keine Koregistrierung der $^{35}Cl^-$ und ^{23}Na-Datensätze durchgeführt. Eine nominelle räumliche Auflösung von $6\,mm^3$ für die ^{35}Cl MRT **a, b**) und von $1{,}9\,mm^3$ für die ^{23}Na MRT **c, d** wurde erreicht. Die gemessene scheinbare Natriumkonzentration des Enchondroms ist mit 255 mmol/l etwa 7-fach höher als die scheinbare Chlorkonzentration mit 36 mmol/l. Die Na^+ und Cl^- Farbskalen besitzen eine unterschiedliche Skalierung. Drei Referenzphantome (offene Pfeile) mit 5 % Agarosegel und verschieden konzentrierter NaCl Lösung (**c** (Na^+) = 154/205/257 mmol/L) sind in der ^{23}Na MRT sichtbar und zwei Referenzphantome (**c** (Cl^-) = 26 mmol/L; links: 4 % Agarosegel; rechts: ohne Agarosegel) sind in der ^{35}Cl MRT sichtbar (offene Pfeile).

importance of chlorine for tumor cell function and progression. In addition, elevated Cl^- concentrations have been observed in muscular channelopathies [3]. Data on the Cl^- content of benign chondroid tumors and their malignant counterparts is very scarce. Using histochemistry with Alcian Blue staining, enchondromas had a similar staining reaction for the $MgCl_2$ concentration to that of adult cartilage [14]. In glioma tissue and in muscle tissue the ratios of the apparent Na^+ to Cl^- concentrations were approximately 2 and 1.2 to 2.0, respectively [2, 3]. In contrast, the measured ratio of the apparent Na^+ to Cl^- concentration was approximately seven in the cartilage forming tumor. This ratio is much higher compared to Na^+ to Cl^- ratios typically found in the fluid spaces of the human body (plasma: 1.4; interstitial fluid: 1.2; intracellular fluid: 1.9) [15]. Various pathophysiologic reasons may explain the different apparent ion concentration levels. For instance, glycosaminoglycans found in cartilage tissue have a high affinity to sodium ions [4] and thus the apparent sodium concentration here is highest among all tissues [16]. Our observation of an apparent Na^+ and Cl^- concentration of the cancellous and cortical bone equal to background noise is in contrast to reports in rats showing a higher sodium content of bone than of muscle tissue [17]. This discrepancy with respect to our in vivo results in humans regarding the measured sodium concentration is most likely caused by invisibility of the ^{23}Na/ ^{35}Cl MRI signals, probably caused by extremely short transverse relaxation times of ^{23}Na and ^{35}Cl in bone tissue. In addition, the continuous analysis of the tumor volume revealed a constant slight growth rate over a period of 14 years. The analysis of growth rates might be helpful for the differentiation between enchondromas and atypical cartilage tumors. However, longitudinal data about the growth of enchondromas is very scarce.

We acknowledge the preliminary nature and limited generalizability of our findings as a limitation given this observation in a single subject. In addition, chlorine and sodium experience a biexponential relaxation with a fast (T_{2f}^*) and a long component (T_{2l}^*), and the very short T_2^* of ^{35}Cl within healthy muscle tissue (T_{2f}^* of 0.37 ms [2]) leads to blurring and a decrease in effective spatial resolution. In particular for ^{35}Cl MRI, the short transverse relaxation times might result in an underestimation of the measured apparent Cl^- concentration. No corrections for differences in relaxation times between references and tumor tissue and no corrections for potential inhomogeneities of the main magnetic (B_0) and transmit field (B_1^+) have been performed. This might reduce the quantitative accuracy [18]. Moreover, for clinical applications, a further breakdown into intra- and extracellular Cl^- concentrations would be desirable. Moreover, for the volumetric measurements, different types of pulse sequences have been used, which might bias the results.

In conclusion, multinuclear 7 Tesla MRI noninvasively reveals interesting information about bone tumor pathophysiology, such as differences in Cl^- and Na^+ homeostasis that could not be visualized on morphological proton MRI. Cartilage-forming tumors like enchondromas obviously have a high contrast-to-noise-ratio when compared with normal bone marrow in ^{23}Na and ^{35}Cl MRI, which may help detection and differentiation in unclear or subtle cases. The discriminative value of non-proton MRI to differentiate between enchondromas and low-grade chondrosarcomas or atypical cartilage tumors has to be analyzed in a prospective study.

Conflict of Interest

The authors declare that they have no conflict of interest.

Acknowledgements

No industry gave support specifically for the study reported in our manuscript. We guarantee that the authors had full control of the data and the information submitted for publication. Moreover, none of the authors is employee of an industrial company. A.M.N. was supported in part by the Helmholtz Alliance Imaging and Curing Environmental Metabolic Diseases (ICEMED), through the Initiative and Networking Fund of the Helmholtz Association. M.A.W. was supported in part by the Eva Luise Köhler Research Award for Rare Diseases (funding was provided for a 7 Tesla ^{35}Cl coil. We have used this coil for pilot experiments, but the coil was not used for the examinations of the present study). A.M.M. was supported by the Deutsche Forschungsgemeinschaft (DFG, project number NA736/2–1).

References

[1] Niesporek SC, Nagel AM, Platt T. Multinuclear MRI at ultrahigh fields. Top Magn Reson Imaging 2019; 28: 173–188

[2] Nagel AM, Lehmann-Horn F, Weber MA et al. In vivo ^{35}Cl MR imaging in humans: a feasibility study. Radiology 2014; 271: 585–595

[3] Weber MA, Nagel AM, Marschar AM et al. 7-T ^{35}Cl and ^{23}Na MR imaging for detection of mutation-dependent alterations in muscular edema and fat fraction with sodium and chloride concentrations in muscular periodic paralyses. Radiology 2016; 280: 848–859

[4] Shapiro EM, Borthakur A, Gougoutas A et al. ^{23}Na MRI accurately measures fixed charge density in articular cartilage. Magn Reson Med 2002; 47: 284–291

[5] Afonso PD, Isaac A, Villagran JM. Chondroid tumors as incidental findings and differential diagnosis between enchondromas and low-grade chondrosarcomas. Semin Musculoskelet Radiol 2019; 23: 3–18

[6] Jurik AG, Hansen BH, Weber K. Solitary enchondromas-diagnosis and surveillance: Danish guidelines. Radiologe 2020; 60 (Suppl. 1): 26–32

[7] Altay M, Bayrakci K, Yildiz Y et al. Secondary chondrosarcoma in cartilage bone tumors: report of 32 patients. J Orthop Sci 2007; 12: 415–423

[8] De Coninck T, Jans L, Sys G et al. Dynamic contrast-enhanced MR imaging for differentiation between enchondroma and chondrosarcoma. Eur Radiol 2013; 23: 3140–3152

[9] Lisson CS, Lisson CG, Flosdorf K et al. Diagnostic value of MRI-based 3D texture analysis for tissue characterisation and discrimination of low-grade chondrosarcoma from enchondroma: a pilot study. Eur Radiol 2018; 28: 468–477

[10] Nagel AM, Bock M, Hartmann C et al. The potential of relaxation-weighted sodium magnetic resonance imaging as demonstrated on brain tumors. Invest Radiol 2011; 46: 539–547

[11] Cuddapah VA, Sontheimer H. Ion channels and transporters [corrected] in cancer. 2. Ion channels and the control of cancer cell migration. Am J Physiol Cell Physiol 2011; 301: C541–C549

[12] Nagel AM, Laun FB, Weber MA et al. Sodium MRI using a density-adapted 3D radial acquisition technique. Magn Reson Med 2009; 62: 1565–1573

[13] Wolf I, Vetter M, Wegner I et al. The medical imaging interaction toolkit. Med Image Anal 2005; 9: 594–604

[14] Kindblom LG, Angervall L. Histochemical characterization of mucosubstances in bone and soft tissue-tumors. Cancer 1975; 36: 985–994

[15] Schmidt RF, Lang F, Heckmann M (eds.) Physiologie des Menschen. 31. Auflage Berlin Heidelberg: Springer; 2011

[16] Madelin G, Lee JS, Regatte RR et al. Sodium MRI: methods and applications. Prog Nucl Magn Reson Spectrosc 2014; 79: 14–47

[17] Winters RW, Whitlock RT, Dewalt JL et al. Effect of alterations of the sodium concentration of the serum upon the content of sodium in bone. Am J Physiol 1958; 195: 697–701

[18] Gerhalter T, Gast LV, Marty B et al. Assessing the variability of ^{23}Na MRI in skeletal muscle tissue: Reproducibility and repeatability of tissue sodium concentration measurements in the lower leg at 3 T. NMR Biomed 2020; 33: e4279